



INTERNATIONAL ATOMIC ENERGY AGENCY
UNITED NATIONS EDUCATIONAL, SCIENTIFIC AND CULTURAL ORGANIZATION
INTERNATIONAL CENTRE FOR THEORETICAL PHYSICS
I.C.T.P., P.O. BOX 586, 34100 TRIESTE, ITALY, CABLE: CENTRATOM TRIESTE



SMR/459 - 4

**SPRING COLLEGE IN CONDENSED MATTER ON:
PHYSICS OF LOW-DIMENSIONAL SEMICONDUCTOR STRUCTURES**

(23 APRIL - 15 JUNE 1990)

**GROWTH OF THIN FILMS AND HETEROSTRUCTURES
OF III-V COMPOUNDS BY MOLECULAR BEAM EPITAXY**

**C.T. FOXON
Philips Research Laboratories
Redhill
Surrey
RM1 5HA
U.K.**

These are preliminary lecture notes, intended only for distribution to participants.

Growth of Thin Films and Heterostructures of III-V Compounds by Molecular Beam Epitaxy

C.T. FOXON AND B.A. JOYCE

1. INTRODUCTION

The technique which has become known as Molecular Beam Epitaxy (MBE) is, at its simplest, a refined form of vacuum evaporation. The molecular beams are produced by evaporation or sublimation from heated liquids or solids contained in crucibles. The flux produced is thus determined by the vapour pressure of the element or compound in the MBE source. At the pressures used in MBE equipment, collision-free beams from the various sources interact chemically on the substrate to form an epitaxially related film. Ultra-high vacuum (UHV) techniques are used to reduce the pressure of gases from the ambient background and thus improve the purity of the layers. More recently gas sources mounted outside the equipment have been employed in what are known respectively as gas source MBE (GS-MBE) - metals plus group V hydrides, metalorganic MBE (MOMBE) - metalorganics plus conventional group Vs and chemical beam epitaxy (CBE) - all gas sources.

MBE began as a basic study of the chemical reactions occurring on surfaces during the growth of III-V compounds but quickly evolved into a practical method for the growth of high purity materials. The ability to start and stop a molecular beam in less than the time taken to grow a single atomic or molecular layer has led to the ability to produce complex multilayer structures. The use of UHV technology has enabled the physical and chemical properties of the films to be measured in-situ using reflection high energy electron diffraction (RHEED) and Auger Electron Spectroscopy (AES). Modulated beam mass spectrometry (MBMS) was developed to study the chemical processes involved and the dynamics of film growth have been investigated using the so-called RHEED oscillation technique which can measure the growth rate in-situ, a unique feature of MBE.

In this series of lectures we will review the fundamental aspects of MBE using mostly examples from the best understood system (Al,Ga)As. We will also discuss the techniques required to grow high purity samples such as high mobility two-dimensional electron gas structures (2DEGs), multi-quantum-well (MQW) structures and superlattices (SL). Finally we will examine the problems associated with dopant incorporation.

2. BASIC TECHNOLOGY OF MBE

Growth rates in MBE are typically about 1 monolayer (ML) per second which is equivalent to a pressure of about 10^{-6} Torr arriving at the sample. For any reasonable purity material to be grown by MBE it is essential to maintain the pressure of unwanted impurities as low as possible (this point will be discussed below in relation to the growth of high mobility structures). MBE requires, therefore, conventional UHV techniques and the apparatus is always constructed to the highest standards of cleanliness. An additional requirement of MBE is that the pressure in the system be low enough to ensure that no gas phase collisions occur. Thus homogeneous reactions, which can occur in MOCVD processes, are entirely avoided and the process is determined entirely by heterogeneous reactions on the substrate surface.

The pumping techniques depend to some extent on the materials being used. In conventional MBE where the group III and V elements are supplied from solid or liquid sources in the MBE equipment, the usual combination employed consists of ion, titanium and closed cycle helium pumps. Following bakeout at about 180°C (limited by the vapour pressure of the group V elements) pressures in the 10^{-11} Torr range are normally obtained. For GSMBE, MOMBE or CBE where the group III or V elements are supplied from gaseous sources an appropriately trapped diffusion or turbomolecular pump may be more suitable to handle the increased gas load on the system. Base pressures in the same range can still be achieved but the partial pressure of hydrocarbons may be somewhat higher.

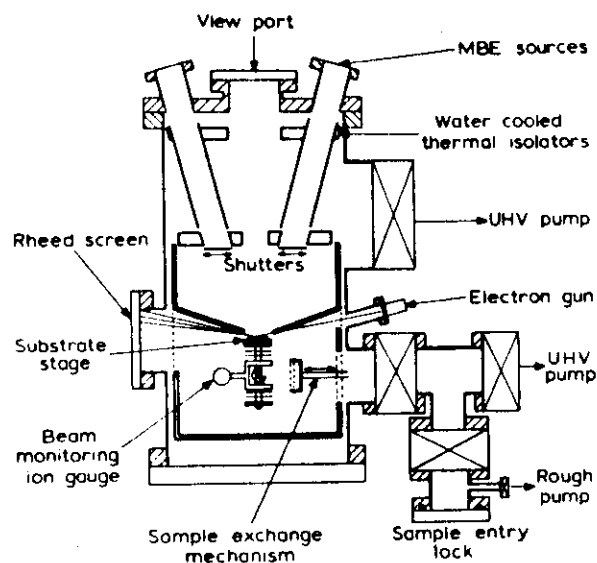


Figure 1: Schematic diagram of an MBE system

The general arrangement of an MBE system is shown schematically in Figure 1. A

the evaporation sources. The low temperature (usually 77K) reduces the arrival rate of unwanted species and provides heat dissipation for both the evaporation sources and the substrate heater.

The evaporation sources, sometimes referred to as Knudsen cells, have a crucible to contain the material. This is now generally made from pyrolytic Boron Nitride (BN), also a III-V compound, but occasionally graphite is also used. Figure 2 shows a true Knudsen source. In this case the crucible has only a small recessed orifice from which the material effuses. This is necessary to ensure that equilibrium vapour pressure is established in the crucible which can be related to the temperature of the source. The cell temperature can be accurately determined by recessing the thermocouple into the crucible taking care to ensure that the heat loss by conduction via the thermocouple leads is negligible compared to the heat received. Spot welding the thermocouple to a large radiation collector can assist in fulfilling this condition. Surrounding the crucible is a heater usually made of Ta wires with BN or Al_2O_3 insulators. Outside the heater are multiple Ta radiation shields. Typically such a source can be heated to 1200°C using quite modest power (about 150 W).

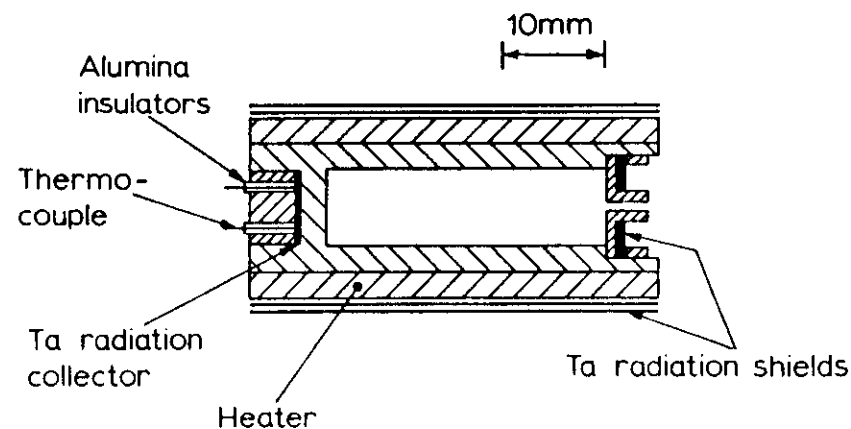


Figure 2: Schematic diagram of a true Knudsen source

From a true Knudsen source with a simple orifice the flux of molecules reaching the sample F , is given by

$$F = 1.118 \times 10^{22} P \times A / [L^2 (M \times T)^{0.5}] \quad (1)$$

where P is the pressure in the source in Torr, A is the area of the orifice in cm^2 , L is the distance from the orifice to the substrate in cm, M is the molecular weight and T the absolute temperature. This relation is obeyed until the point where the mean free path becomes comparable to or less than the diameter of the orifice. Above this pressure (temperature) there is a transition from molecular flow to viscous flow. In conventional MBE this limit is never exceeded but in GSMBE and CBE it is closely approached for the group V sources.

In a practical MBE system a true Knudsen source is seldom used, since by increasing the size of the orifice it is possible to reduce the melt temperature required to give a particular flux at the substrate. This in turn will reduce the power consumption and minimise the number of unwanted impurities associated with outgassing of the cell and its surroundings. In such a source there is no unique relation between temperature T and flux F but from RHEED measurements we can directly determine the fluxes of the group III and V elements (see below). The prime requirement is for a stable reproducible flux and typically over an 8 hour day less than 1% drift is observed with day to day variations of 2 to 5%. Increasing the orifice diameter reduces the pressure within the source and therefore increases the mean free path for the molecules, this ensures molecular flow is maintained.

To start and stop the molecular beams a simple mechanical shutter can be used, typically this can operate in a time short (0.1 to 0.3s) compared to the time taken to deposit a ML (1s). Two practical problems arise; the first comes from the need to operate the shutter many thousands of times for superlattice samples leading to occasional vacuum (bellows) failures; the second point is that the shutter is a heat shield for the source and flux transients associated with the opening of the shutter are often observed. Both lead to problems in growing short period MQW or SL samples.

To obtain crystalline material of adequate quality it is usually essential to heat the substrate to a temperature of between 400 and 700°C. This is usually achieved using a heater which remains within the vacuum system. In some MBE systems the sample is attached to a platen using liquid In and the platen is heated by radiation, but with more recent designs the sample is heated radiatively. III-V compounds are, however, transparent to radiation below the bandgap and this therefore leads to poor coupling.

Since the fluxes from the various MBE sources come from different directions their distributions across the substrate will differ and this can lead to films of non uniform thickness and composition. In practice this can be overcome by rotating the substrate during growth, ideally once per monolayer of material deposited. This is simple in principle but difficult to achieve in practice because no conventional lubricant can be used on the various bearings. The bellows motion usually used to transmit the rotation has also to be capable of many million rotations. One of the major advantages of MOMBE and CBE may be that a uniform flux can be obtained over a large area without the need to rotate the sample.

Sample introduction is via a two or three chamber system. In the first chamber the pressure is reduced to about 10^{-4} Torr using sorption pumps. These are then isolated and an ion pump or small cryopump is used to reach $<10^{-6}$ Torr. The sample is then transferred to the second part of the interlock in which water vapour is removed by heating the sample to about 400°C, the limit is set by the temperature at which the III-V compound begins to decompose. After about one hour the pressure in this second chamber is usually below 2×10^{-10} Torr. At this stage the sample can be safely introduced into the growth chamber without degrading the vacuum quality.

In practical MBE systems the diagnostics used are relatively simple. A quadrupole

been achieved. Leak checking before and after the system bakeout is essential and if a QUAD is mounted in the preparation chamber it can be used to ensure that all the water vapour is removed from the sample before transfer to the growth chamber.

A RHEED facility in the growth chamber is also used to determine that the native oxides have been removed before growth and to determine the growth rates for the various binary compounds (see below). This is usually carried out on a small monitor slice kept in the preparation chamber. The RHEED system consists of a 10 to 15 keV electron gun on one side of the chamber with a phosphor screen on a window on the other side. The detection system will be discussed below.

The final item found in most MBE systems is a beam monitoring ion gauge which can be placed in the sample position to measure the intensity of the molecular beams. The absolute sensitivity of the gauge depends to some extent on the materials being deposited on the collector and so cannot easily be used in a quantitative way, but the relative sensitivity to different species is usually maintained and it is a useful tool where RHEED measurements cannot easily be employed.

3. FUNDAMENTAL ASPECTS OF MBE

Several experimental and theoretical investigations have contributed to our present understanding of the processes controlling the growth of films and dopant incorporation in MBE: surface chemical processes have been studied using MBMS methods (Foxon et al 1974), the dynamics of film growth have been examined using the RHEED technique (Joyce et al 1988) and Monte-Carlo (M-C) simulations of growth have added to our knowledge of the factors influencing growth and interface roughness (Madhukar and Ghaisas 1988). In addition thermodynamic calculations have shown fundamental limitations involved in using certain dopants and the factors governing the incorporation of unwanted impurities (Heckingbottom 1985).

MBMS studies

The principle of MBMS is illustrated in Figure 3. By mechanically modulating the molecular beams arriving at, or leaving, the sample surface we are able to distinguish "real" signals in the mass spectrometer from "false" ones arising due to background gases in the vacuum system in the vicinity of the ioniser. By modulating desorbing fluxes (case (a) shown in Figure 3) we are able to determine desorption rates, sticking coefficients, thermal accommodation coefficients of surface species and the order of chemical reactions. If instead we modulate the incident beam (case (b) in Figure 3) we can also determine surface lifetimes and from the temperature dependence deduce binding energies of adsorbates. From such data we can build up a fairly complete picture of the chemistry of the growth process. It is important to note that any species which exist only on the surface will not be detected by this technique, which could be a problem in applying these methods to the study of MOMBE or CBE.

Principle of modulated molecular beam measurements

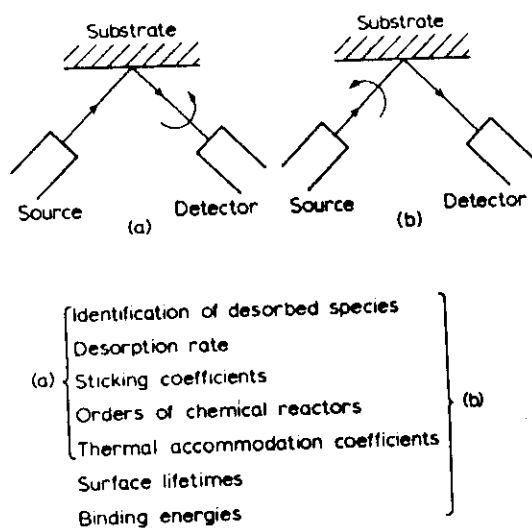
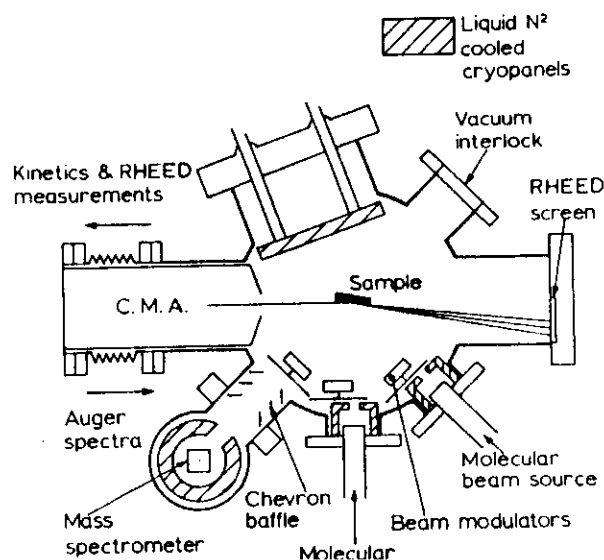


Figure 3: MBMS principle

The type of experimental arrangement used is illustrated schematically in Figure 4. It is a conventional UHV MBE equipment with additional facilities for mechanically modulating the incident and desorbing beams (1 to 100Hz); the detector (Quadrupole Mass Spectrometer - QUAD) is arranged as a single pass density detector, i.e. any molecule not being ionised is condensed on the 77K panel. RHEED and AES facilities may also be included.



We will consider as a typical example the reaction features involved in the growth of GaAs films on GaAs (001) substrates, for incident beams of Ga with either As_2 or As_4 (Foxon and Joyce 1975, 1977).

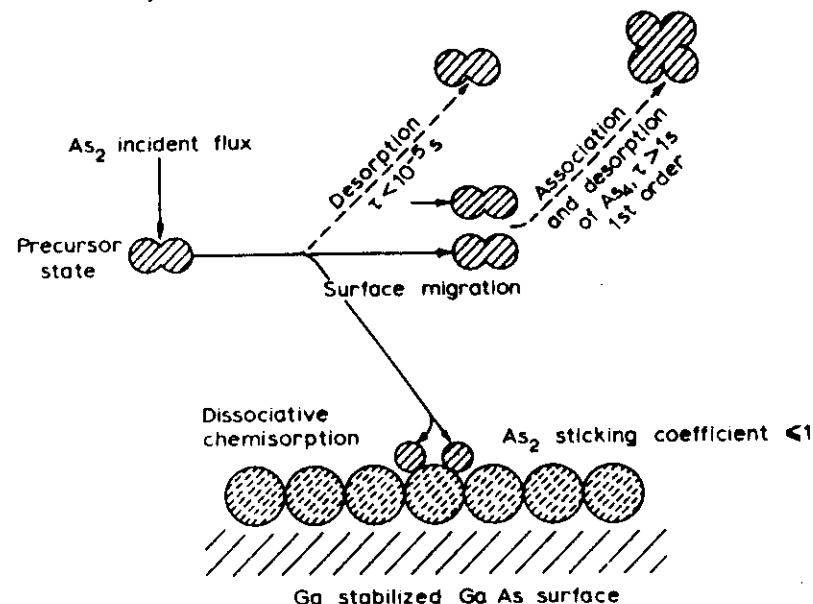


Figure 5: Model of the growth chemistry of GaAs from molecular beams of Ga and As_2

The interactions of an As_2 flux and gallium on a GaAs substrate are summarised in the growth model shown in Figure 5. The As_2 molecules are first adsorbed into a mobile, weakly bound precursor state. The surface residence time of molecules in this state is less than 10^{-5} s. The basic process for As incorporation during thin film growth is a simple first-order dissociative chemisorption on surface Ga atoms. The maximum value of the As_2 sticking coefficient is unity, which is obtained when the surface is covered with a complete monolayer of Ga atoms (as in Figure 5). At relatively low substrate temperatures ($< 600\text{K}$) there is an additional association reaction to form As_4 molecules. These desorb very slowly by a first order reaction. At substrate temperatures above 600K some dissociation of GaAs may occur.

By contrast, the reaction mechanism with an incident As_4 flux is significantly more complex. The model for this is shown in Figure 6. Here the As_4 molecules are first absorbed into a mobile precursor state. The migration of the adsorbed As_4 molecules has an activation energy of about 0.25 eV. The surface residence time is temperature dependent, from which a desorption energy of about 0.4eV may be determined. A crucial finding is that the sticking coefficient of arsenic never exceeds 0.5, even when the Ga flux is much higher than the As_4 flux or when the surface is completely covered with a monolayer of Ga atoms (as in Figure 6). This is explained by assuming a pairwise dissociation of As_4 molecules chemisorbed on adjacent Ga atoms. This

flux. From any two As_4 molecules four As atoms are incorporated in the GaAs lattice, while the other four desorb as an As_4 molecule.

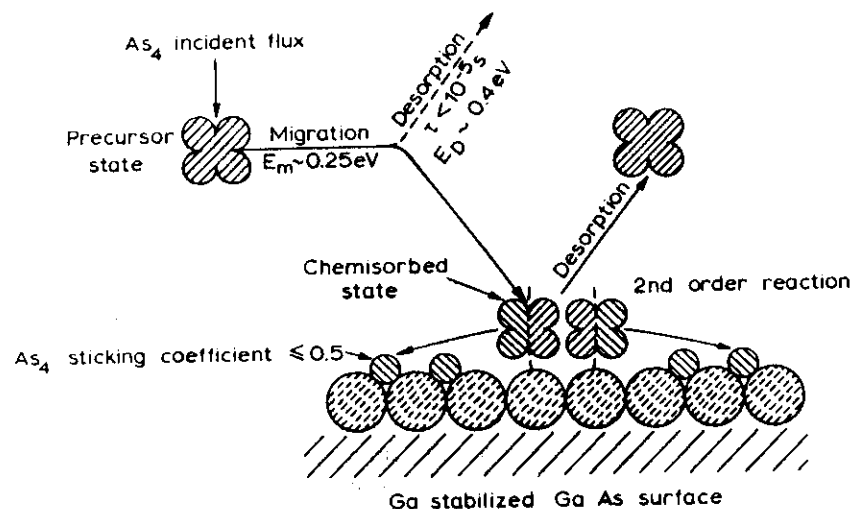


Figure 6: Model of the growth chemistry of GaAs from molecular beams of Ga and As_4 .

The different chemistry is reflected in the properties of GaAs films grown from As_2 and As_4 . In general, for equivalent growth conditions As_2 -grown films have lower deep level concentrations and better optical (photoluminescence and interface recombination velocity) properties than those grown from As_4 .

Although well over ten years old, these models are still the accepted versions and have in fact received some recent experimental support. Tsao et al (1988) measured changes in sticking coefficient of As_4 (not the As incorporation rate, as they claimed) by a non-modulated beam desorption method which relied on extensive cryopumping to separate beam from background signals in the mass spectrometer. (The As incorporation rate involves the formation of Ga-As bonds in the proper lattice site and this cannot be measured mass spectrometrically). They found no temporal oscillatory behaviour in the signal, which is consistent with the measured chemical process being fast compared with the incorporation rate of As into the lattice via layer-by-layer growth (We will return to this point for a more detailed discussion when we consider growth dynamics). They found, however, in agreement with Foxon and Joyce (1975), a maximum As_4 sticking coefficient of 0.5 and were also able to establish that the surface reconstruction changed from (001)- 2×4 to (001)- 4×2 just when the sticking coefficient reaches this maximum value, i.e. the surface stoichiometry becomes more Ga-rich.

Harbison and Farrel (1988) have proposed totally speculative configurational models

GaAs-(001) from elemental beams. The models are based on consideration of the electron occupancy of surface bonds, but since they have no experimental justification and in fact conflict with existing data obtained by RHEED and angle resolved photoemission spectroscopy (Larsen et al 1982) we prefer not to include them here.

Kinetic effects in alloy growth

For alloys with mixed Group III elements (i.e. $\text{III}_a\text{III}_b\text{V}$), reactions with the Group V element are identical to those observed in binary compound growth, so we are only concerned with those factors which influence the Group III ratio. We should note, however, that the thermal stability of the alloy, once produced, is determined by the less stable of the two binary compound end members from which it is formed. In $(\text{Al,Ga})\text{As}$, for example, the thermal stability of GaAs is the limiting factor. This is beautifully demonstrated by the work of Kawai et al (1986), who showed that the Langmuir (free) evaporation of $(\text{Al,Ga})\text{As}$ at 750°C proceeds by the selective evaporation of GaAs until four monolayers of AlAs have accumulated at the surface, when sublimation ceases.

At low growth temperatures, the alloy composition is determined only by the flux ratio, since the sticking coefficients are effectively unity. Where growth is carried out at higher temperatures, which is often necessary to obtain optimum electrical or optical properties, this is no longer the case. The temperature dependence of their sticking

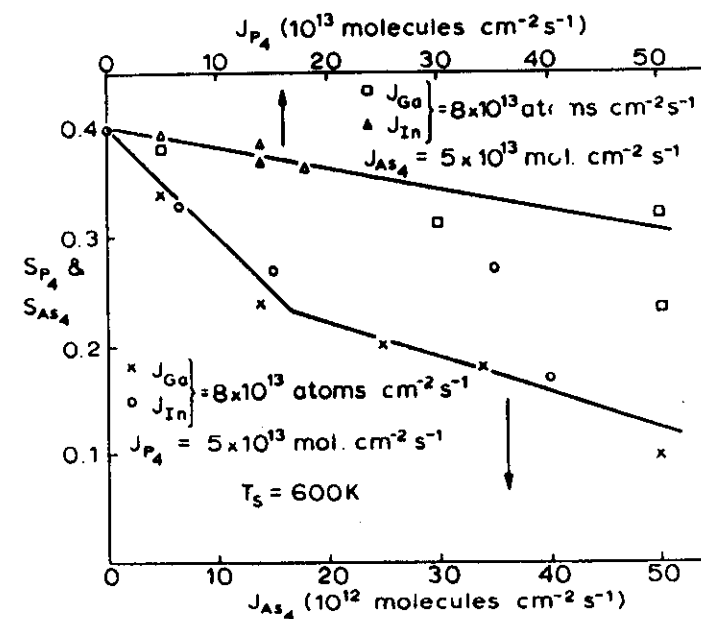


Figure 7: Sticking coefficient of $\text{As}_4(P_4)$ as a function of the $P_4(As_4)$ flux at constant fluxes of Ga or In at $T_s = 600 \text{ K}$

coefficients relates closely to that of their vapour pressure, which can therefore be used as an adequate guide to composition control under conditions which correspond to the Group III-rich liquidus. Contrary to some literature reports, the presence of one element does not significantly influence the sticking coefficient of the other during growth.

For mixed Group V element alloys (i.e. III $V_x V_y$) the situation is much more complex. There is no simple relationship between flux (either of dimers or tetramers) and film composition, because one element is always adsorbed much more readily than the other, the order being $Sb > As > P$ (Chang et al 1977, Foxon et al 1980). This is illustrated in Figure 7 for As_4 and P_4 and is shown as the influence of one molecule on the sticking coefficient of the other, but no serious attempt has been made to understand the mechanism. To control film composition the strongly adsorbed component is supplied in the required ratio to the Group III element and the weakly adsorbed component is provided in excess. The method can break down at high temperature, however, where in, say, $Ga(As,P)$, As_2 is lost preferentially by thermal dissociation but tends to be replaced by phosphorus, which is present in excess (Woodbridge et al 1982).

Growth from gaseous compound sources - MOMBE and CBE

One of the more significant changes in technology is the use of gas sources for the preparation of III-V compounds, referred to as chemical beam epitaxy (CBE) or metal-organic molecular beam epitaxy (MOMBE) or gas source molecular beam epitaxy (GSMBE). Advantages include non-depleting sources which can be changed or recharged from outside the UHV system; no heat source in the growth chamber other than the substrate; uniform layer thickness and doping levels without substrate rotation and reduced surface defect density.

At present, the sources used are Group V hydrides, i.e. PH_3 and AsH_3 , with Group III alkyls, principally trimethyls and triethyls. The major disadvantage of these materials is their high toxicity and pyrophoricity, so considerable attention is being given to the preparation and purification of alternative precursors. These include compounds which contain both the Group III and Group V atoms in the same molecule and in the correct ratio to produce stoichiometric films, while also being volatile and non-toxic.

Although very high quality material has been prepared from alkyl and hydride sources, with good control of layer thickness and doping precision, little or no work has been carried out on the chemistry of the growth process, which is clearly much more complex than that occurring with elemental sources. Experimental approaches have all relied simply on measurement of the growth rate as a function of substrate temperature and incident fluxes. Such information is useful for empiric process control, but provides little insight into reaction mechanisms and pathways.

Several underlying concepts can be emphasised however, the most important of which is that since growth occurs in the molecular flow regime, there are no gas phase collisions; the beams impinge directly on to the substrate. This is quite different from

reactions have been claimed to play an important part, even in the so-called low pressure regime, since flow is still viscous. Some very recent results by Aspnes et al (1988) cast serious doubts on the extent of gas phase decomposition during atmospheric pressure MOCVD. They used in situ reflectance difference spectroscopy to follow the surface coverage of TMG and found the kinetic limits to growth to be determined by surface site availability and subsequent decomposition of TMG. Their experimental approach precluded the possibility of a gas phase component of the decomposition reaction, but the results were nevertheless in excellent agreement with literature values where no attempts were made to restrict possible homogeneous reactions. It is therefore not clear to what extent an understanding of one process implies any understanding of the other.

A second, related factor is that the hydrides do not appear to have adequate dissociation rates on the substrate surface and it is necessary to predissociate them so that they impinge predominantly in the form of elemental dimers. The alkyls, however, require no predissociation and are allowed to impinge directly; nor do they require the presence of Group V species to enable them to dissociate, but the rate is temperature dependent. As determined only from film growth rate measurements, the dissociation rate increases to a maximum with increasing temperature and then decreases rather rapidly as the temperature is further increased. This appears to be generally true, but the exact shape of the curve is dependant on the particular compounds involved.

A third pointer to possible mechanisms is the dependence of carbon incorporation into the growing film on the particular alkyl used. In the case of GaAs, it is well-established that very much higher concentrations of carbon are incorporated from trimethyl gallium (TMG) than from triethyl (TEG). It is assumed that the use of TEG allows the possibility of a reaction pathway for surface decomposition of the metal triethyl via β -hydrogen elimination to form ethene, which of course cannot occur with TMG.

Robertson et al (1988) have attempted to model the flux and temperature dependence of the growth rate of GaAs from beams of TEG and As_2 (derived from AsH_3). In the absence of any experimental information on surface or desorbing species, surface reaction kinetics or mechanisms, they assume the adsorbed molecules to be mono-, di- and triethyl gallium, together with ethyl radicals and the rate limiting step is supposed to be cleavage of the second ethyl-gallium bond. β -hydrogen elimination from adsorbed ethyl groups to form ethene is also assumed, as is Arrhenius behaviour of rate constants for the elementary reaction steps. The observed non-linear dependence of growth rate on flux is then associated with a second order recombination of adsorbed diethyl gallium with an ethyl radical, followed by desorption of triethyl gallium. The high temperature decrease in growth rate is ascribed to desorption of diethyl gallium. Such speculative approaches are clearly of limited value; kinetic and spectroscopic measurements are essential if any real progress is to be made in understanding the complex surface processes involved in MOMBE (CBE).

4. SURFACE STUDIES

MBE is a unique thin film growth process in that it is UHV based and therefore compatible with a wide range of surface chemical and physical techniques. It also allows in-situ growth of a number of structures not otherwise accessible.

Crystallography and Composition

In general semiconductor surfaces either relax by bond rotation or reconstruct, i.e. display a lower symmetry than that produced by a simple termination of the bulk lattice. In III-V compounds the form of the reconstruction is related to surface stoichiometry. We will treat GaAs(001) as a typical example. It is a polar orientation and the surface is ideally terminated by a complete layer of Ga or As atoms (i.e. it is composed of alternating layers of covalently bonded Ga and As atoms, Figure 8, but a wide range of stoichiometry and structure can occur. The different structures in order of decreasing Ga surface concentration are C(8x2), (otherwise 4x2), 3x1 and 2x4 (otherwise C(2x8)), with high temperatures and high Ga fluxes favouring a high Ga surface population. A particular reconstruction can exist over a moderately wide surface composition range ($\approx 10\%$), but there is an additional structure, the C(4x4), formed by chemisorption of excess arsenic, which has a much wider range, with As present at well over monolayer coverage.

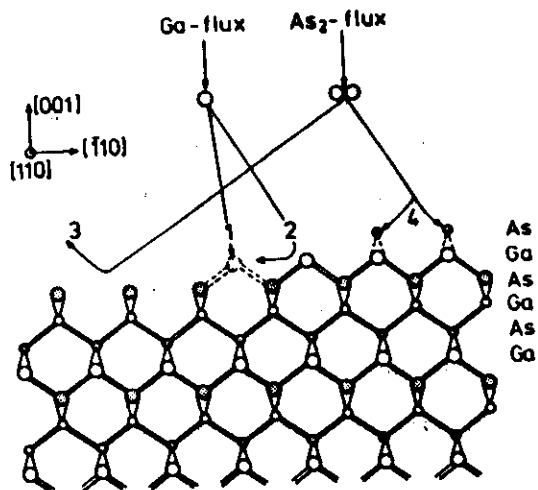


Figure 8: Schematic model of a GaAs (001), showing alternate layers of Ga and As build-up of surface stoichiometry during growth.

Surface crystallography is most conveniently monitored by electron diffraction techniques. Low-energy diffraction (LEED), which uses a back-scattering geometry, techniques. Low-energy diffraction (LEED), which uses a back-scattering geometry, techniques. Low-energy diffraction (LEED), which uses a back-scattering geometry, techniques.

combination with MBE. For this, the forward scattering geometry of RHEED is more appropriate, since the electron beam is at extreme grazing incidence, whereas the molecular beams impinge almost normally on the substrate. Although the same basic information is obtained from both methods, a combination of RHEED and MBE enables the surface crystallography to be monitored even under dynamic conditions when the surface is growing.



Figure 9: RHEED patterns from two orthogonal $\langle 110 \rangle$ azimuths of the GaAs (001) - 2x4 reconstructed surface

As an example of the information which can be obtained from RHEED we consider the GaAs(100) surface. Figure 9 shows the RHEED patterns in two-orthogonal $\langle 110 \rangle$ azimuths from a 2x4 reconstructed surface, one with a twofold and the other with a fourfold increase in periodicity. In addition to establishing the surface geometry, the RHEED pattern can also be used to evaluate the surface morphology (surface steps, facets, antisite disorder, etc.).

5. GROWTH DYNAMICS

The in-situ investigation of thin film growth dynamics has been made possible recently by the discovery and development of the RHEED intensity oscillation technique (Neave et al 1983, Van Hove et al 1983, Joyce et al 1988), which has proved extremely valuable for MBE and to a lesser extent for gas source beam techniques (Chiu et al 1987).

The primary observation is that damped oscillations occur in the intensity of all features of the RHEED pattern immediately following the start of growth. A typical data set for the growth of a GaAs(001) oriented film is shown in Figure 10 taken using the specular spot on the 00 rod. The steady state period corresponds precisely to the growth of a single molecular layer, i.e. a complete layer of Ga(Al) + As atoms, equivalent to $a_s/2$ in the [001] direction. Oscillatory response to a surface sensitive

probe during thin film deposition is generally considered to be the manifestation of a two dimensional layer-by-layer growth mode. Similar results have been reported from a number of techniques, including LEED (Horn and Henzler 1987), helium atom scattering (Gomez et al 1985), and AES (Namba et al 1981), but will not be discussed here.

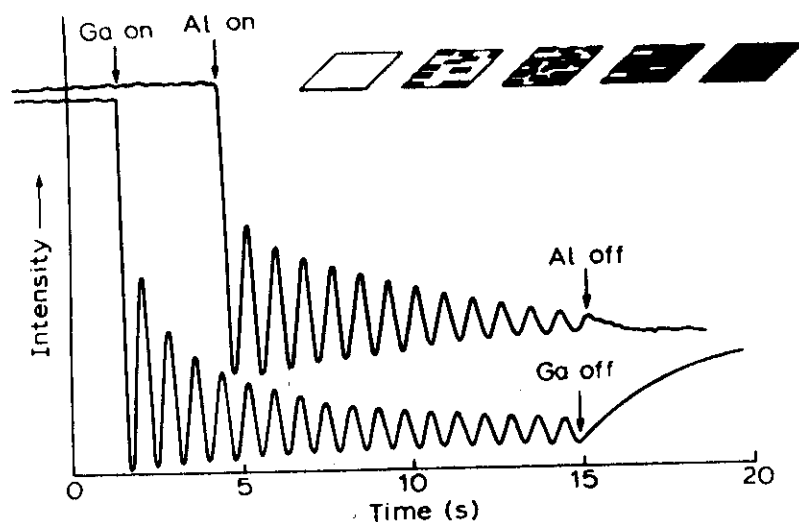
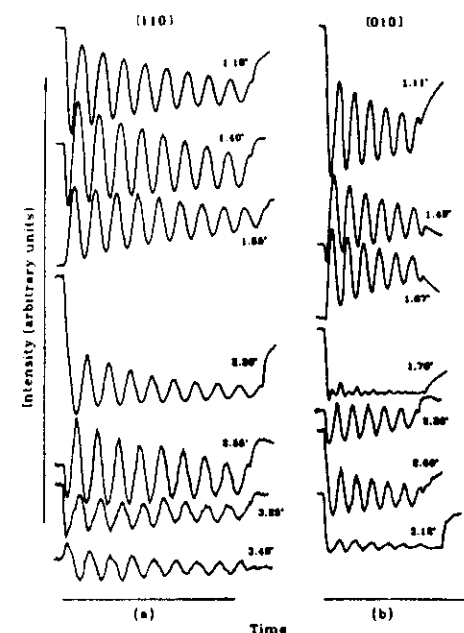


Figure 10: Intensity oscillations of the specular beam in the RHEED pattern from a AlAs and GaAs (001) - 2x4 surface during film growth.

Common to all models proposed to explain the oscillatory intensity response is the assertion that it occurs as a direct result of the changing surface topography associated with a layer-by-layer growth mode (Neave et al 1983). To examine this concept in more detail, we need to establish the nature of the diffraction processes contributing to the measured intensity, most usually made at the position of the specular beam on the 00 rod. Diffraction under the conditions used is a multiple scattering process and the elastic component of the specular intensity is attributed mainly to multiple diffraction and surface resonances. In addition, however, there is a very significant contribution from inelastic and/or incoherent processes, with the proportion of each (elastic and inelastic) depending on polar and azimuthal angles and beam energy. The primary and elastically diffracted beams undergo stronger diffuse scattering in the surface layer as it becomes disordered (assumes a higher step density) during growth. Diffusely scattered electrons which penetrate into the bulk can also be subsequently Bragg scattered and emerge as Kikuchi features, which are observed more strongly during growth than from a static surface.

Oscillations recorded under different diffraction conditions will therefore show the

Figure 11, which shows oscillations from the specular spot on the 00 rod as a function of polar angle for [110] and [010] azimuths at a constant energy of 12.5 keV. The growing film was GaAs on a GaAs(001)-2x4 reconstructed surface, which was maintained throughout by using a temperature of 580°C, a Ga flux of 1×10^{14} atoms $\text{cm}^{-2} \text{s}^{-1}$ and an arsenic (As_2) flux of 2×10^{14} molecules $\text{cm}^{-2} \text{s}^{-1}$. There is clearly a wide range of oscillation waveforms, but the growth conditions were invariant, so the differences must be attributed to diffraction, not growth effects. The most important



Provided that due regard is paid to diffraction effects, it is nevertheless possible to obtain considerable insight into growth behaviour from RHEED observations. Absolute growth and evaporation rates, alloy composition, growth modes, adatom migration, surface relaxation and interface formation can all be investigated.

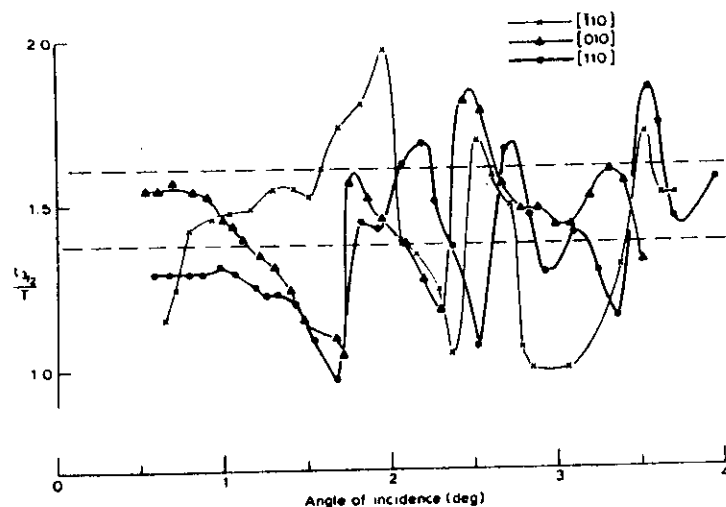


Figure 12: Phase relationships of RHEED oscillations as a function of the polar angle for different azimuths from a GaAs(001)-2x4 reconstructed surface. The growth conditions were constant as for Fig. 9. Phase is defined at the time taken to reach the second minimum normalized by the time of a complete period.

Growth and evaporation rates: the layer-by-layer mode

These measurements depend only on the steady state oscillation period, which is a high precision absolute rate monitor for layer-by-layer growth (Neave et al 1983, Van Hove et al 1983) or evaporation (Kojima et al 1985, Van Hove and Cohen 1985). Alloy composition ($\text{III}_x\text{III}_{1-x}\text{V}$) can also be determined in situ and this is especially important for high temperature growth where sticking coefficients of the Group III atoms are not always unity.

Apparently identical RHEED intensity oscillations have also been observed during the growth of GaAs from TEG and AsH_3 (Chiu et al 1987) and of InP from trimethyl indium and phosphine (Morishita et al 1988). Their presence certainly implies a two-dimensional layer-by-layer growth mode, but there must be doubt whether electron beam stimulated dissociation of the alkyls influences the actual growth rate.

Adatom migration during growth

The occurrence of a layer-by-layer growth mode implies that there must be substantial adatom surface migration. It is also well established (Foxon and Joyce 1975, 1977) that the Group III element flux is growth-rate controlling and this enables its surface migration behaviour to be determined from RHEED intensity oscillations (Neave et al 1985). The principle is a very simple extension to vicinal plane growth, illustrated in Figure 13.

The substrate is slightly misoriented in a specific direction by a known amount from a low index plane (singular surface) and by assuming that this vicinal surface will adopt a minimum energy configuration by breaking up into low index terraces separated by monatomic steps, an average step-free width l is defined. If the migration length of the Group III element is λ , for $\lambda > l$ the step edge will act as the major sink for migrating adatoms and there will be no two dimensional (2-D) growth on the terrace. Since RHEED intensity oscillations only occur as the result of 2-D growth, they will be absent for this growth mode. If, however, growth conditions are varied to the point where $\lambda < l$, 2-D growth will occur on the terraces and oscillations will be observed. It is therefore comparatively simple to study λ as a function of growth conditions.

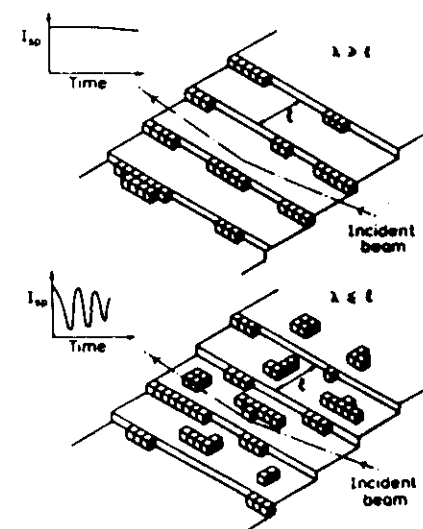


Figure 13: Schematic illustration of the principle of the vicinal plane method, showing the change in RHEED information as the growth mode changes from step propagation to 2-D growth.

It must be emphasized that in this context, surface migration refers to the transport of Ga adatoms in a weakly bound precursor state before final incorporation in a lattice site. Once such a site is reached, migration is assumed to have ceased. Incorporation is not a reversible process (at normal growth temperatures).

Ideally, the measurements should be performed by systematically varying the extent of misorientation and hence terrace width, but in practice it is simpler to use a single substrate with a known misorientation and vary the migration length by changing growth parameters. A typical data set obtained at fixed As_2 and Ga fluxes by varying the substrate temperature is shown in Figure 14.

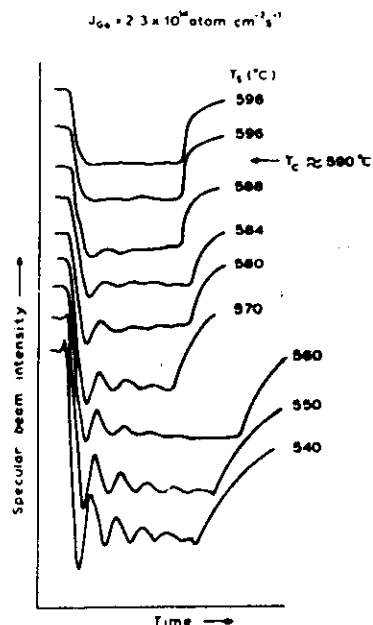


Figure 14: Data set showing the transition from oscillations to constant response as a function of substrate temperature, with constant J_{Ga}

If we assume that surface migration is isotropic, it is in principle possible to determine values of the surface migration coefficient D_0 and the activation energy of surface migration E_0 using the relationships:-

$$\chi^2 = 2 D \tau \quad (2)$$

and

$$D = D_0 \exp (-E_0/kT) \quad (3)$$

Here χ is the mean displacement (terrace width), D the migration coefficient at a temperature T and τ is the surface lifetime in the precursor state. The choice of a value for τ is unfortunately not a simple matter.

Conventionally (Neave et al 1985, Van Hove and Cohen 1987) it has been equated to the monolayer deposition rate ($\tau = N_s/J$, where N_s is the number of surface sites per

unit area and J the Group III atom flux) but this is certainly an oversimplification and at best represents an upper limit. Nishinaga and Cho (1988) have proposed an alternative approach, based on classical nucleation theory, which therefore requires large critical nuclei appropriate to a thermodynamic treatment involving surface free energy concepts. For typical MBE growth conditions however, the critical nucleus is likely to be a single adatom, so the reliability of a thermodynamic approach must also be questioned.

By equating τ with monolayer deposition rate as a working hypothesis, it is possible to determine an energy value, E_0 , from the temperature dependence of the disappearance of oscillations at different Group III atom fluxes. A value of $\approx 1.3\text{eV}$ was obtained by Neave et al (1985). This is not the migration energy alone, but includes a term representing bonds made by the atom with its nearest neighbours, E_n .

$$\text{Then } E_0 = E_n + E_p, \quad (4)$$

so E_0 , the activation energy of migration, will be considerably less than 1.3eV , which seems reasonable given the essential role of surface migration in 2-D growth. It is important to realise, however, that migration parameters are not fundamental constants, they are involved in the kinetics, not thermodynamics of crystal growth and are pertinent only to adatom migration under specific growth conditions.

In spite of these quantitative difficulties, there is good evidence for a model in which growth is two-dimensional until the adatom migration length becomes less than the steady state mean terrace width, when step propagation becomes the dominant mode. It is implicit in this model that the observed damping of the oscillations is a measure of the transition to steady state, which is assumed to have been reached when the oscillation amplitude becomes zero.

Surface relaxation and growth technique modifications

If growth is stopped by shutting of the Group III flux whilst maintaining constant the substrate temperature and Group V flux, the commonly observed effect (Neave et al 1983) is for the intensity of the specular spot in the RHEED pattern to "recover" almost to its pre-growth value in a manner dependent on the precise point in the intensity oscillation at which the shutter is closed (Lewis et al 1985). The increasing intensity has been equated with "smoothing" of the surface, i.e. terrace widths increase. In general terms the "recovery" or relaxation occurs in two stages (fast and slow) and obeys an expression of the form:

$$I = A_0 + A_1 \exp (-t/\tau_1) + A_2 \exp (-t/\tau_2) \quad (5)$$

where τ_1 and τ_2 are the temperature dependent time constants of the fast and slow stages respectively. For GaAs(001) 2x4, Neave et al (1983) reported an activation energy of $\approx 2\text{eV}$ associated with the rapid initial stage, possibly related to Ga-As bond dissociation at step edges. From their Monte Carlo simulation, Clarke and Vvedensky (1989) have proposed that during the fast stage two dimensional islands lose any

from sites with the lowest co-ordination. The slow step then results from adatom clusters evolving to form the maximum number of nearest neighbour bonds.

The development of the final surface morphology achieved by relaxation will depend critically on the stage in the monolayer deposition at which growth is stopped. In studying the phenomenon using RHEED, therefore, it is clearly essential to choose diffraction conditions where maxima correspond to monolayer completion (Joyce et al 1988).

The fact that termination (or interruption) of growth can lead to surface smoothing by a process of dissociation of two-dimensional islands, followed by surface diffusion and reformation in a lower energy configuration has given rise to a number of alternative forms of MBE growth. The modifications were introduced with the idea of growing more "perfect" interfaces in heterojunctions, quantum wells and superlattices, i.e. maximizing areas of single composition in the interface plane, or minimizing the number of layers normal to this plane in which compositional variations occur. They include interrupted growth (Madhukar et al 1985, Sakaki et al 1985), atomic layer epitaxy, ALE (Briones et al 1987) and migration enhanced epitaxy, MEE (Horikoshi et al 1988). In essence, however, they all rely on some form of interruption of one or other or both (anion and cation) fluxes.

In the simplest version of growth interruption, the shutter of the Group III cell, but not the Group V, is closed briefly (up to 60s) to allow the specular RHEED beam intensity to recover to its initial value. It is almost certain that this will result in a lower step density and it is likely to be more successful for lower binding energy, faster diffusing species, so, for example a considerably lower temperature is required for a GaAs layer than for AlAs or (Al,Ga)As (Tanaka and Sakaki, 1988). Its efficacy will also be critically dependent on the point in the monolayer when growth is interrupted, so correct choice of diffraction conditions is vital. Both ALE and MEE involve periodic interruptions of both fluxes during growth. ALE is based on an alternate supply of constituent elements to the substrate surface, regulated so that a single complete layer is provided with each pulse. This is not a problem for the Group V species, since their adsorption is self-regulated by the available Group III atoms in the surface. This is not so for the Group III atoms, however and an excess can accumulate as the free element on the surface if the amount per pulse is too large. This can be obviated by the use of RHEED, and provided correct diffraction conditions are used, exact monolayer quantities can be supplied. The results appear to indicate that "high quality material" can be prepared at rather lower temperatures than by conventional growth, but it should be remembered that the overall growth rate is low in ALE and it would be more valid to make a comparison with material grown conventionally at this rate and temperature. This information is not yet available. The basic mechanism seems to be a rapid relaxation process as the result of briefly interrupting growth very close to monolayer completion.

The MEE process also involves the alternating supply of cation and anion fluxes and it is claimed that by reducing the surface concentration of the Group V element during the impingement of the Group III atoms the latter's surface migration rate is enhanced, resulting in a smoother, higher quality growth at low temperatures. Again a better

description would probably be that only very short relaxation times are required near monolayer completion and the alternating supply allows this to happen.

One final point needs to be raised about MEE, however. It is demonstrated that the observed RHEED intensity oscillations persist throughout the whole growth, even for relatively thick films and they are essentially undamped. This is claimed to be indicative of high quality growth, in contradistinction to conventional MBE, where oscillations tend to damp relatively quickly.

Two factors need stressing: in conventional growth, damped oscillations merely indicate a change of growth mode from two-dimensional to step propagation, and are not necessarily associated with material quality, only with step distribution and migration lengths. Much more importantly, though, the origin of the oscillations recorded in MEE is quite different from that for conventional growth. In MEE the oscillations occur simply because there is a transient change in surface reconstruction from a Group III stable form to a Group V stable form with each alternate pulse and the specular intensity is a strong function of surface reconstruction (Larsen et al 1986).

Growth modifications are thus seen to be an interesting approach to producing smoother interfaces and lower temperature growth. The mechanisms of ALE and MEE probably relate more to enhanced relaxation from near-complete monolayers than to enhanced adatom migration and in MEE in particular the RHEED intensity oscillations are associated with reconstruction effects, not the growth mode.

6. GROWTH OF HIGH PURITY STRUCTURES BY MBE

Typical growth rates for MBE are about 1MLs^{-1} or $1\mu\text{m}$ per hour. This corresponds to a pressure of about 1×10^{-6} Torr for the group III species at the sample surface. To achieve high purity material, therefore, it is essential to keep the partial pressure of gases which stick to a minimum (for $N_d + N_a < 10^{15}\text{ cm}^{-3}$ we need $P_{\text{imp}} < 10^{-13}$ Torr assuming a unity sticking coefficient). The way we achieve this is to outgas thoroughly the sources prior to loading, use the best possible start materials and then bake the system extensively to remove water vapour. Full details of the methods we use have been published elsewhere (Foxon and Harris 1986).

For both GaAs bulk films and for two-dimensional-electron-gases (2DEGs) we find a progressive improvement in the properties of the films grown by MBE as the growth sequence continues after the system loading and bakeout. This is because background impurities which limit purity are gettered by the growth process and their concentration is gradually reduced providing there is no external leak in the system.

Bulk GaAs

Using this technique we have grown several thick intentionally doped GaAs films with electron mobilities at 77K of $> 1 \times 10^5$ and a best value of $1.33 \times 10^5\text{ cm}^2\text{ V}^{-1}\text{ s}^{-1}$. The free electron concentrations were about $2 \times 10^{16}\text{ cm}^{-3}$. This suggests the background acceptor concentration in our material is below $2 \times 10^{14}\text{ cm}^{-3}$. Recently we have

reported an undoped GaAs film, grown using a superlattice prelayer, which at low temperature has luminescence dominated by free exciton emission (t'Hooft et al 1987).

2DEGs

For 2DEGs, the structure we have used for our high mobility samples is shown in Figure 15. The GaAs buffer is grown starting at 580°C, increasing gradually to 630°C. The Si flux is calibrated to give a doping level in GaAs of $2 \times 10^{18} \text{ cm}^{-3}$, which in (Al,Ga)As gives a Si concentration of $1.33 \times 10^{18} \text{ cm}^{-3}$. The undoped GaAs cap is to aid the contact technology by preventing oxidation.

If we consider a realistic picture of the 2DEG band diagram then for narrow spacers, $d < 100 \text{ \AA}$, the mobility will be determined by ionised impurity scattering near the 2DEG. For wider spacers, $\sim 400 \text{ \AA}$, the ionised impurities near the surface (10x the number near to the 2DEG) will have a significant contribution and reducing or moving these should improve the measured mobility. For very wide spacer samples, with $d > 800 \text{ \AA}$, the background impurity of the GaAs will be the key factor in determining the mobility.

Figure 16 shows the results of a systematic set of samples in which only the undoped spacer layer thickness was intentionally varied. The general form of the curve is as expected, with a peak mobility for $d \sim 600 \text{ \AA}$. The drop in mobility at large spacer thicknesses occurs because reducing the 2DEG density results in a lower Fermi velocity and hence mobility, for a fixed scattering rate. Increasing the thickness of the doped region of (Al,Ga)As and hence removing some of the ionised impurities near the surface resulted in a 50% improvement in peak mobility, as expected.

GaAs 170 Å undoped		
Al _{0.32} Ga _{0.68} As 400(500) Å $1.3 \times 10^{18} \text{ cm}^{-3} \text{ (n)}$		
Al _{0.32} Ga _{0.68} As d Å undoped		
<hr/>		
2DEG		
GaAs 4 μm undoped		
<hr/>		
GaAs Substrate undoped		

Figure 15: Structure of high mobility 2DEG samples

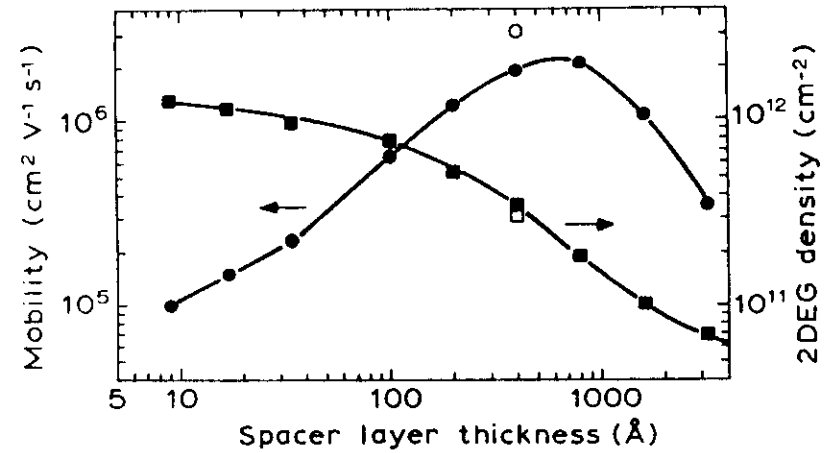


Figure 16: Effect of undoped spacer layer thickness on the density and mobility of 2DEG structures

For several years the best reported mobilities for 2DEG samples were approximately $2 \times 10^6 \text{ cm}^2 \text{ V}^{-1} \text{ s}^{-1}$ at a sheet carrier density of about $5 \times 10^{11} \text{ cm}^{-2}$. In our studies we were able to obtain similar mobility material at somewhat lower electron densities, as shown in Figure 16 (Foxon et al 1986) and by optimising the structure obtained mobilities of $3 \times 10^6 \text{ V}^{-1} \text{ s}^{-1}$ at 4K (Harris et al 1986, 1987). Using a prelayer to improve the background scattering in the GaAs English et al (1987) obtained a 2DEG with a mobility at $< 2 \text{ K}$ of $5 \times 10^6 \text{ cm}^2 \text{ V}^{-1} \text{ s}^{-1}$ at a sheet carrier density of $1.6 \times 10^{11} \text{ cm}^{-2}$. More recently even higher mobilities have been achieved at 4K over a wide range of electron densities (Foxon et al 1989). This has been achieved by combining the optimum structure for the doped regions (Harris et al 1987) with the use of a superlattice to trap impurities (t'Hooft et al 1987).

Qualitatively we can account well for the observed dependence of mobility on spacer layer thickness but quantitatively theories still predict lower mobilities than are observed in experimental measurements.

For the structures discussed above, where the (Al,Ga)As layers are grown on GaAs (the so called "normal" structure) very high mobility 2DEGs can be obtained, but if the layer sequence is reversed and GaAs is grown on doped (Al,Ga)As (the so called "inverted" structure) much lower mobilities are observed. Various factors have been suggested for this inferior performance including interface roughness (Alexandre et al 1986), impurity build-up during the growth of (Al,Ga)As which is deposited in the GaAs near the 2DEG (Alexandre et al 1986) Si migration from the doped (Al,Ga)As into the GaAs either by diffusion or segregation (Inoue et al 1985, Gonzales et al 1986), (this point will be discussed in more detail below) and scattering from band-edge discontinuity fluctuations at the interface (Cho et al 1987). We have recently identified a new factor, electron localisation at the interface (Airaksinen et al 1988).

The structure of the samples grown for this study are shown in Figure 17. The 2DEG is formed in a narrow QW doped only on the surface side to avoid problems of Si migration. In sample C, GaAs is grown on bulk (Al,Ga)As but in sample D the alloy is replaced by a short period SL of equivalent band-gap. In this experiment any difference in mobility can only relate to the quality of the inverted interface.

For a conventional "normal" 2DEG structure we observe a monotonic increase in mobility as the sample is cooled from 300 to 4K with the carrier concentration being essentially constant. For sample C we observe a strong decrease in both mobility and carrier concentration as we go to low temperatures, but for sample D we observe behaviour typical of a 2DEG with a 22A spacer.

Gold (1986) has recently predicted that a metal-insulator transition can occur in quantum well structures due to electron localisation by a randomly fluctuating potential. Strong localisation arises when the magnitude of the potential fluctuations exceeds the Fermi energy of the carriers as shown in Figure 18. By reducing the size of the fluctuations (by replacing the alloy with a superlattice) we were able to recover in sample D normal 2DEG behaviour. To test this idea further, additional samples of type D but with wider undoped spacers (lower 2DEG density) were grown. For a 40A spacer sample, conducting behaviour was still observed after illumination but the 100 and 200A spacer samples were completely insulating. We were thus able to estimate the size of the potential fluctuations to be about 30meV.

Sample C	Sample D
170A undoped GaAs	
400A (Al,Ga)As $1.5 \times 10^{18} \text{ cm}^{-3}$	
22A undoped (Al,Ga)As	
150A GaAs QW	
0.5 micron thick	
(Al,Ga)As alloy	AlAs/GaAs superlattice
0.5 micron undoped GaAs	

Figure 17: Structure of QW samples used to investigate the quality of the inverted interface

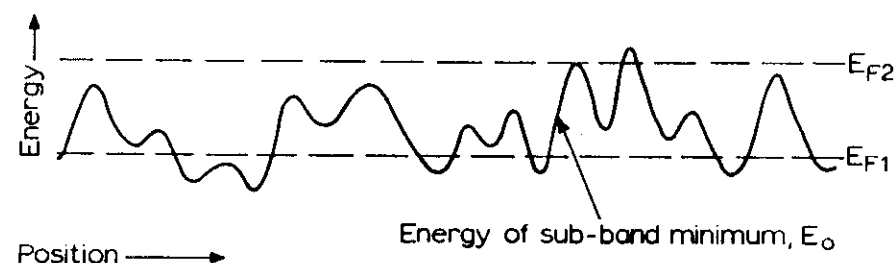


Figure 18: Illustration of how strong localisation occurs due to local potential fluctuations

The improved properties of the inverted interface obtained by replacing the alloy with a superlattice still do not give an interface of comparable quality to the "normal" interface under the growth conditions we have used.

7. QUANTUM WELLS (QWs) AND SUPERLATTICES (SLs)

Further insight into the quality of interfaces can be obtained by studying the physical properties of undoped QWs and SLs grown under essentially identical conditions. Figure 19 shows a cross-sectional TEM micrograph of a GaAs-AlAs SL comprising alternate layers 3 monolayers thick. Similar micrographs of a 2 + 2 ML SL can also be observed but at present 1 + 1 ML SLs cannot be resolved. Two features are evident from such micrographs; the first is that averaged over the depth of the film, interfaces abrupt on a scale of less than 1 monolayer can be produced; and secondly there is a general tendency for the wavy interfaces initially obtained to smooth out as growth proceeds. The mechanism responsible for this gradual improvement is not clear at present but the reduction of interface energy may be a factor.

By modelling the integrated intensities of the satellite reflections, X-ray diffractometry from MQW and SL structures can also give us valuable information on the lateral extent of the interfaces. From such studies estimates of interface roughness from 1 to 4ML have been proposed, with one interface (probably the GaAs on AlAs or (Al,Ga)As) extending over a larger distance in the growth direction.

Most information on the quality of the interfaces has been obtained from low temperature photoluminescence (excitation) (PL/PLE) studies of QWs and SLs. Here the key point to remember is that the spacing of interface steps λ in relation to the

diameter, D , of the exciton determines what will be observed in PL/PLE. When $\lambda \ll D$ a pseudo-smooth interface will be obtained and when $\lambda \gg D$ we have a truly-smooth heterojunction. If $\lambda \sim D$ excitons will be trapped at the interface and the energies of specific recombination peaks in PL will be lower than the corresponding



Figure 19: TEM micrograph of a GaAs(3 μ m)/AlAs(3 μ m) superlattice

positions in PLE, the so-called Stokes shift. In PL/PLE studies of QWs there are often examples of multiple peaks. In some cases they correspond to monolayer differences in well width at the upper "normal" interface (Deveaud et al 1984), but there are other examples in the literature (Bajaj et al 1986) where the authors correctly point out that the fine structure observed cannot correspond to QWs differing in width by an integer number of monolayers. It is important to point out that in the case of MQWs interwell width fluctuations due to variations in growth rate for example can give rise to such multiple peaks but studies of the temperature dependence of the PL/PLE rule out this explanation in the case referred to above.

The structural integrity of SLs can be studied using PL/PLE to give further information on the quality of heterointerfaces. We have recently shown that for GaAs-AlAs SLs grown at 630°C alloy like behaviour is observed for $n = m = 1$ or 2 ML but for $n = m > 3$ ML true superlattices are formed with electronic properties quite different from those observed in $\text{Al}_{0.5}\text{Ga}_{0.5}\text{As}$ films grown under identical conditions (Moore et al 1988). This is entirely consistent with the X-ray data presented above which suggests an inverted interface extending over a few MLs. To produce "true" $1 + 1$ or $2 + 2$ ML SLs modified growth procedures will be needed.

8. DOPANT INCORPORATION

The choice of suitable p and n dopants is of crucial importance in exploiting MBE as a production technique for devices such as HEMTs, lasers etc..

The group VI elements suffer from a tendency to surface segregate when supplied in elemental form, which may be related to the fact that they evaporate in part as dimers. This problem can be overcome by using compound sources such as PbTe which dissociates to give Te atoms (readily incorporated at low temperatures) plus Pb atoms which are weakly bound to the surface and lost by re-evaporation. Above about 600°C, however, the group VI elements are also lost by re-evaporation and therefore not appropriate for most device structures.

The group II elements fall into two categories, Zn and Cd have too high a vapour pressure to be retained at typical growth temperature. Be and Mg do not suffer from this problem, but Mg is so highly reactive that it was difficult to obtain electrically active material in early MBE equipment and Be therefore has been almost universally used as the p type dopant in MBE.

The group IV element Ge is amphoteric and is therefore not a suitable n type dopant, Sn suffers from kinetically limited surface segregation which leaves Si as the most universally used n type dopant.

Synthesis of particular doping profiles can in principle be achieved by changing the temperature of the Si or Be cell to give the required flux as a function of time, but the thermal response time of the furnace limits the rate of change to about a decade in

(Wood et al 1980). Here dopant is deposited during a growth interruption, the group III shutters are closed but the As flux is used to maintain the surface stoichiometry. By appropriate choice of dopant flux and interval any arbitrary profile can be synthesised.

This idea was extended to include the concept of "delta" doping (Zrenner et al 1984) in which the dopant atoms are deposited on a single plane to form a novel 2DEG system. This is different from the 2DEG systems formed at heterojunctions in that there is no large spatial separation of electrons and ionised impurities so that in this system extremely high mobilities are not obtained. The system is nevertheless interesting because very much higher sheet carrier concentrations can be obtained ($\sim 10^{13} \text{ cm}^{-2}$ cf $\sim 10^{11} \text{ cm}^{-2}$ in (Al,Ga)As/GaAs 2DEGs) and many more subbands can be occupied in the potential well formed by the dopant atoms (4 and 7 subbands at 4×10^{12} and 10^{13} cm^{-2} respectively, Ploog 1987).

In both "atomic-plane" and "delta" doping the absence of any arriving group III element means that the number of Ga dangling bonds in the surface is minimised. For amphoteric dopants like Si and Ge this has the effect of reducing the number incorporated onto the As sublattice and reducing their tendency towards compensation. For Si, choosing alternative substrate orientations can increase the incorporation on the As sublattice and in fact p type material has been obtained on 211A or 311A Ga terminated surfaces (Wang et al 1985).

Both Si and Be suffer from a number of additional problems and neither is an ideal dopant source. Both show enhanced diffusivity at high doping levels (Gonzales et al 1986, Devine et al 1987). Here above a critical level the diffusion mechanism changes and as a result MQW or SL structures can become disordered. It is possible to see this directly in TEM micrographs of heavily doped samples.

For both Si and Be it has also been suggested that surface segregation is a problem. This has recently been studied using delta doped samples (Beall et al 1988). Ultra-high resolution SIMS measurements on Si delta doped GaAs samples have shown that there is evidence of surface segregation at temperatures above 550°C with a characteristic segregation length of around 50 to 100 Å (close to conventional SIMS resolution limits). This is occasionally masked by very high diffusivity observed at doping levels $> 2 \times 10^{18} \text{ cm}^{-3}$. Key evidence in favour of segregation came from experiments where in conventionally doped films the substrate temperature was suddenly decreased, resulting in a doping spike as predicted by the segregation model, and a corresponding dip on increasing the temperature as expected. So far no convincing evidence for Be segregation has been obtained.

Despite the difficulties associated with Si and Be they can be employed to provide suitably doped films as evidenced by their use in MBE production of HEMTs (Fujitsu), lasers (ROHM) and high speed microwave devices (Philips).

9. ACKNOWLEDGEMENTS

We would like to thank our many colleagues at both Philips Research Laboratories and the Interdisciplinary Research Centre for Semiconductor Materials for their contributions to the work outlined in this article.

REFERENCES

- Airaksinen J M, Harris J J, Lacklison D E, Beall R B, Hilton D, Foxon C T and Battersby S J 1988 *J. Vac. Sci. Technol.* **B6** 1151
- Alexandre F, Lievin J L, Meynadier M H and Delalande C 1986 *Surface Sci.* **168** 454
- Aspens D E, Colas A, Stedma A A, Bhat R, Koza M A and Keramidias V G 1988 *Phys. Rev. Lett.* **61** 2782
- Bajaj K K, Reynolds D C, Litton C W, Singh J, Yu P W, Masselink W T, Fischer R and Morkoc H 1986 *Solid State Comm.* **29** 215
- Beall R B, Harris J J and Clegg J B 1988 *Semi. Sci. Technol.* **3** 612
- Briones F, Gonzalez L, Recio M and Vaquez M 1987 *Japan J. Appl. Phys.* **26** L1125
- Chang C A, Ludeke R, Chang L L and Esaki L 1977 *Appl. Phys. Lett.* **31** 759
- Chiu T H, Tsang W T, Cunningham J E and Robertson A 1987 *J. Appl. Phys.* **62** 2302
- Cho N M, Ogale S B and Madhurkar A 1987 *Appl. Phys. Lett.* **51** 1016
- Clarke S and Vvedensky D D 1989 *J. Crystal Growth* in the press
- Deveaud B, Emery J Y, Chomette A, Lambert B and Baudet M 1986 *Appl. Phys. Lett.* **45** 1078
- Devine R L S, Foxon C T, Joyce B A, Clegg B A and Gowers J P 1987 *Appl. Phys.* **A44** 195
- English J H, Gossard A C, Stormer H L and Baldwin K W 1987 *Appl. Phys. Lett.* **50** 1826
- Foxon C T, Boudry M R and Joyce B A 1974 *Surface Sci.* **44** 69
- Foxon C T and Harris J J 1986 *Philips J. Res.* **41** 313
- Foxon C T, Harris J J, Hilton D, Hewett J and Roberts C, *Semi. Sci. and Technol.* to be published.
- Foxon C T, Harris J J, Wheeler R G and Lacklison D E 1986 *J. Vac. Sci. Technol.*, **B4** 511
- Foxon C T and Joyce B A 1975 *Surface Sci.* **50** 434
- Foxon C T and Joyce B A 1977 *Surface Sci.* **64** 293
- Foxon C T, Joyce B A and Norris M T 1980 *J. Crystal Grow* **49** 132
- Gold A 1986 *Solid State Comm.* **60** 531
- Gomez L J, Bourgeat S, Ibanez J and Salmaron M 1985 *Phys. Rev.* **B31** 2551
- Gonzales L, Clegg J B, Hilton D, Gowers J P, Foxon C T and Joyce B A 1986 *Appl. Phys.* **A41** 237
- Harbison J P and Farrell H H 1988 *J. Vac. Sci. Technol.* **B6** 733
- Harris J J, Foxon C T, Barnham K W J, Lacklison D E, Hewett J and White C 1987 *J. Appl. Phys.* **61** 1219

- Harris J J, Foxon C T, Lacklison D E and Barnham K W J 1986 Superlattices and Microstructures **2** 563
- Heckingbottom R 1985 Molecular Beam Epitaxy and Heterostructures, ed. Chang L L and Ploog K Martinus Nijhoff, Holland pp 71-104
- Horn M and Henzier M 1987 J. Crystal Growth **81** 428
- Horikoshi Y, Kawashima M and Yamaguchi H 1988 Japan J. Appl. Phys. **27** 169
- Inoue K, Sakaki H, Yoshino J 1985 Appl. Phys. Lett. **46** 973
- Joyce B A, Neave J H, Zhang J and Dobson P J 1988 Reflection High Energy Diffraction and Reflection Electron Imaging of Surfaces ed. Larsen P K and Dobson P J, Plenum, pp 397-417
- Kawai N J, Kojima T, Sato F, Sakamoto T, Nakagawa T and Ohta K 1986 12th Int. Symp. on GaAs and Related Compounds IOP Conf. Ser. **79** Adam Hilger pp 433
- Kojima T, Kawai N J, Nakagawa T, Ohta K, Sakamoto T and Kawashima M 1985 Appl. Phys. Lett. **47** 726
- Larsen P K, Dobson P J, Neave J H, Joyce B A, Bolger B and Zhang J 1986 Surface Sci. **169** 176
- Larsen P K, Van der Veen J F, Mazur A, Pollman J, Neave J H and Joyce B A 1982 Phys. Rev. **B26** 3222
- Lewis B F, Greenhaver F J, Madhurkar A, Lee T C and Fernandy R 1985 J. Vac. Sci. Technol. **B3** 1317
- Madhukar A and Ghaisas S V 1988 CRC Critical Reviews in Solid State and Materials Science **14** 1
- Madhukar A, Lee T C, Yen M Y, Chen P, Kim J Y, Ghaisas S V and Newman P G 1985 Appl. Phys. Lett. **46** 1148
- Moore K H, Duggan G, Dawson P and Foxon C T 1988 Phys. Rev. **B38** 5535
- Morishita Y, Maruno S, Gotada M, Nomeva Y and Ogata H 1988 Appl. Phys. Lett. **52** 42
- Namba Y, Vook R W and Chao S S 1981 Surface Sci. **109** 320
- Neave J H, Joyce B A, Dobson P J and Norton N 1983 Appl. Phys. **A31** 1
- Neave J H, Dobson P J, Joyce B A and Zhang J 1985 Appl. Phys. Lett. **47** 100
- Nishinaga T and Cho K 1988 Japan J. Appl. Phys. **27** L12
- Ploog K 1987 J. Crystal Growth **81** 304
- Robertson A, Chiu T H, Tsang W T and Cunningham J E 1988 J. Appl. Phys. **64** 877
- Sasaki H, Tanaka M and Yoshino J 1985 Japan J. Appl. Phys. **24** L417
- Tanaka M and Sakaki H 1988, Superlattices and Microstruct. **4** 237
- Thooft G W, Van der Poel W A J A, Molenkamp L W and Foxon C T 1987 Phys. Rev. **B35** 8281
- Tsao J Y, Brennan T M and Hammons B E 1988 Appl. Phys. Lett. **53** 288
- Van Hove J M and Cohen P I 1985 Appl. Phys. Lett. **47** 726
- Van Hove J M, Lent C S, Pukite P R and Cohen P I 1983 J. Vac. Sci. Technol. **B1** 741
- Van Hove J M and Cohen P I 1987 J. Cryst. Growth **81** 13
- Wang W I, Mendex E E, Kuan T S and Esaki L 1985 Appl. Phys. Lett. **47** 826
- Wood C E C, Metzger G, Berry J and Eastman L F 1980 J. Appl. Phys. **51** 383
- Woodbridge K, Gowers J P and Joyce B A 1982 J. Crystal Growth **60** 21
- Zrenner A, Reisinger H, Koch F and Ploog K 1984 Proc. 17th Int. Conf. on Phys. of Semiconductors, ed. W A Springer, Berlin 1985 325

Scanning Electron Microscopy (SEM)

Microcharacterisation of Semiconducting Materials and Devices

D B HOLT

Characterisation refers to the complete range of techniques used in determining the structure and properties of semiconducting materials, multilayer structures and devices. It therefore includes (i) the diffraction techniques used for determining crystal structures, (ii) the microscopic techniques for determining defect microstructure and (iii) the physical measurement techniques for determining (volume averaged) values of physical properties.

The SEM (scanning electron microscope) techniques provide measurement with a micron scale resolution and so can determine defect microstructures and local values of physical properties. The term microcharacterization has come into use to emphasise this dual character of SEM techniques.

SEMs outsell TEMs (transmission electron microscopes) by 3 to 1 worldwide despite the fact that TEMs have much better (lateral, spatial) resolution and have highly developed interpretive theories available. Clearly, therefore, SEMs must have great advantages to offset this. One practical advantage is that SEMs can be used to examine macroscopic specimens with little or no special preparation, e.g. whole wafers or electronic devices can be inspected. Moreover, SEMs offer not only lateral, spatial resolution but also depth resolution, spectral (signal) resolution, time resolution, etc.

However, the big advantages of SEMs are those outlined in the next section. The advantages of the scanning principle are so great that many further types of scanning microscope are now appearing such as scanning laser and acoustic microscopes and scanning facilities have been incorporated into TEMs to produce "analytical" TEMs or TEMSCANS.

Scanning Electron Microscopy

The scanning electron microscope (SEM) is powerful and versatile because

- (i) it has six modes of operation which provide information about many different groups of properties of solid objects and
- (ii) the information is obtained essentially as electrical signals suitable for electronic data processing to provide quantitative values of many different properties as well as for presentation in various types of micrographs.

The SEM is, therefore, not only a family of different kinds of microscopes, it is also a family of microanalytical measuring systems. Its performance parameters depend on the

